JOURNAL OF VIROLOGY, Nov. 2006, p. 11409–11415 Vol. 80, No. 22
0022-538X/06/$08.00+0 doi:10.1128/JVI.00234-06

Selection of Early-Occurring Mutations Dictates Hormone-Independent Progression in Mouse Mammary Tumor Lines[▽]

Albana Gattelli,[1,2] María N. Zimberlin,[1,2] Roberto P. Meiss,[2]
Lucio H. Castilla,[3] and Edith C. Kordon[1,2]*

IFIBYNE and ILEX (CONICET), Facultad de Ciencias Exactas y Naturales, UBA, (1428) Buenos Aires,[1] and IIHEMA and IEO, Academia Nacional de Medicina, (1425) Buenos Aires,[2] Argentina, and Program in Gene Function and Expression, University of Massachusetts Medical School, Worcester, Massachusetts 01605[3]

Received 1 February 2006/Accepted 30 August 2006

Mice harboring three mouse mammary tumor virus (MMTV) variants develop pregnancy-dependent (PD) tumors that progress to pregnancy-independent (PI) behavior through successive passages. Herein, we identified 10 predominant insertions in PI transplants from 8 independent tumor lines. These mutations were also detected in small cell populations in the early PD passages. In addition, we identified a new viral insertion upstream of the gene *Rspo3*, which is overexpressed in three of the eight independent tumor lines and codes for a protein very similar to the recently described protein encoded by *Int7*. This study suggests that during progression towards hormone independence, clonal expansion of cells with specific mutations might be more relevant than the occurrence of new MMTV insertions.

The mechanisms underlying breast cancer progression can be studied using mouse models susceptible to developing mammary tumors. With the BALB/c strain, three recently discovered mouse mammary tumor virus (MMTV) variants (BALB/2, BALB/14, and LA) induce pregnancy-dependent (PD) mammary tumors (4, 10), which eventually progress to a pregnancy-independent (PI) behavior. Infected pregnant females were examined in order to detect pregnancy-dependent primary tumors. Individual tumors (tumor area, ~50 mm^2) were minced in sterile phosphate-buffered saline, and randomized fragments of 1 to 2 mm^3 were transplanted subcutaneously by trocar in the flanks of syngeneic females that were either maintained in a virginal state or crossbred. Three to eight consecutive tumor passages were made in order to investigate their eventual progression to pregnancy independence. We have previously shown that PD tumors frequently arise as polyclonal populations, while their PI derivatives appear in subsequent transplant generations as monoclonal cell populations. In addition, the latter frequently display MMTV insertions undetected in the corresponding PD by Southern blot analysis (3).

To evaluate the relevance of MMTV retroviral insertions for tumorigenesis with our model, we estimated the amount of exogenous MMTV provirus in mouse mammary gland and primary tumor DNA by quantitative PCR (qPCR) analysis. Genomic DNA was extracted as previously described (9), and amplifications were performed using viral strain-specific primers (10). Two-month-old virgin female mammary glands showed low provirus content, and in several cases, we were not able to detect the BALB/2 and BALB/14 MMTV variants. However, a significant increase was observed in the three viral strains when DNA from multiparous females (after the third pregnancy) was analyzed (Fig. 1A). Interestingly, proviral levels remained similar or even decreased either after more pregnancies or in primary tumors (Fig. 1A). Since we have found no evidences of unintegrated proviral DNA in our samples, these results suggest that MMTV mutational capacity could have reached a maximum after the third pregnancy, i.e., before virus-associated aberrant morphology may be detected. However, we cannot be sure that progenitor cells, which would be privileged targets for tumor development (13), have accumulated the maximum of provirus integration at that stage. We may be detecting proviral DNA mostly from fully committed highly infected alveolar cells, which will probably undergo apoptosis during involution. These cells are not prone to becoming neoplastic. Alternatively, progenitor cells may acquire MMTV insertions more slowly and require more pregnancies to change their pattern of behavior, even though a smaller number of mutations in this particular set of cells would be more significant for tumor development.

MMTV-infected virgin female mammary glands exhibited no significant sign of abnormal development and a very low number of infiltrating lymphocytes. However, an augmentation of these cells was observed after three or more pregnancies, mainly in peri- and intralobuloacinar unit patterns. Then, the proviral content observed in the virgin gland would be mostly due to the epithelial compartment, while in the parous gland the presence of virally infected lymphocytes might provide a minor contribution to the exogenous MMTV levels.

Parous normal glands and primary tumors did not harbor a predominant proviral variant. However, a single MMTV variant prevailed in the latter passages of most (11/16) in vivo tumor lines. Based on this, specific primers that did not hybridize with MMTV-endogenous sequences were used to amplify MMTV insertion sites identified by Southern blot analysis in PI transplants of eight tumor lines (Fig. 1B). Ten MMTV proviral insertions were cloned out by inverse PCR (IPCR) (5,

* Corresponding author. Mailing address: IFIBYNE-CONICET, Facultad de Ciencias Exactas y Naturales, UBA Ciudad Universitaria, Pabellón 2, 2do piso, (1428) Buenos Aires, Argentina. Phone: 5411-4576-3300/09, ext. 483/213. Fax: 5411-4576-3321. E-mail: ekordon@qb.fcen.uba.ar.

▽ Published ahead of print on 13 September 2006.

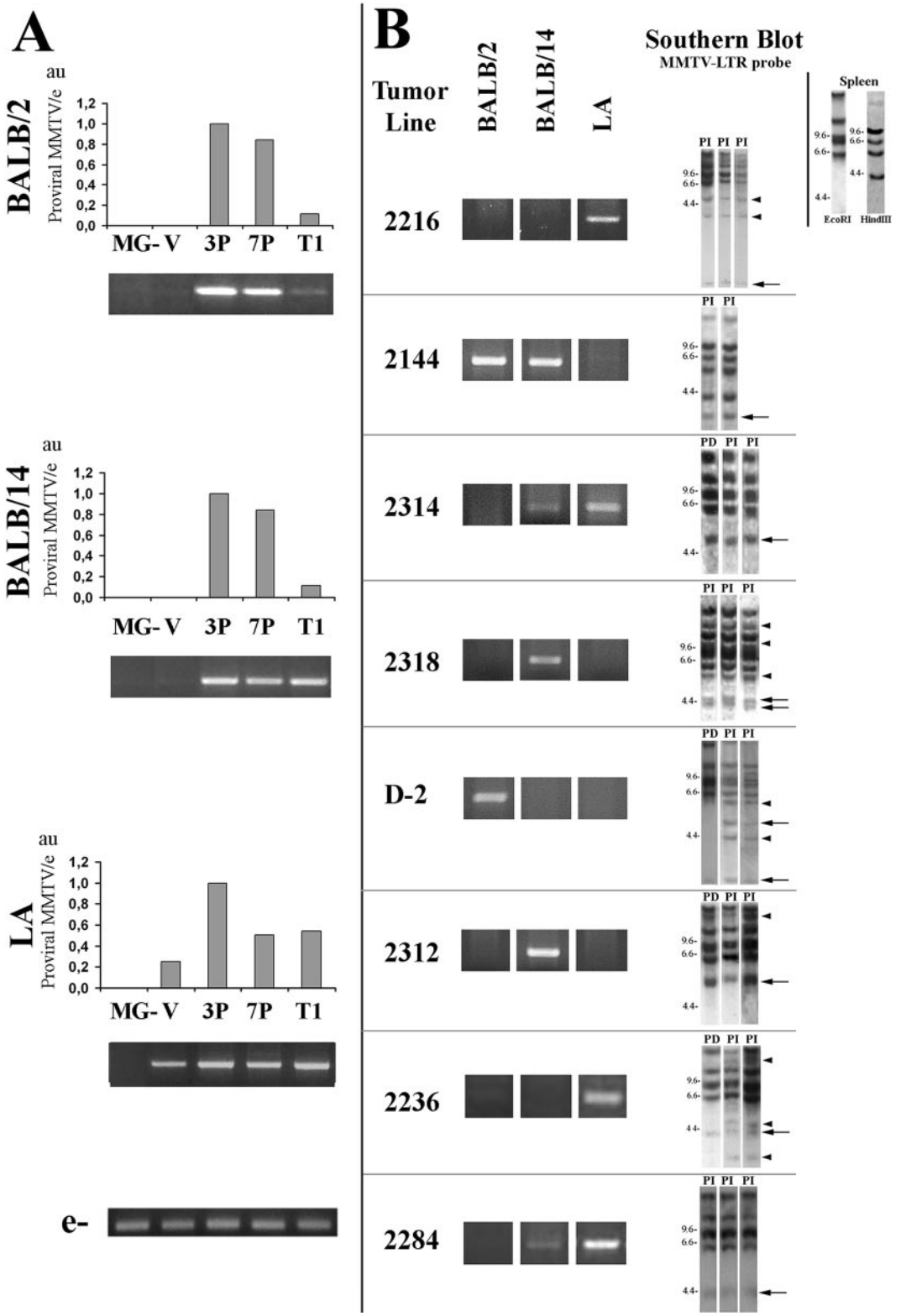

FIG. 1. Proviral MMTV content in normal mammary glands and tumors. Viral strain-specific PCR products (BALB/2, BALB/14, and LA; primers shown in Table 1) were obtained from DNA of the following: (A) MMTV-uninfected normal mammary glands (MG), MMTV-infected mammary glands from virgin females (V), females after third pregnancy (3P) or after seventh pregnancy (7P), and primary mammary tumors (T1); (B) pregnancy-independent passages from eight different tumor lines. For A and B, each bar graphic and ethidium bromide-stained gel shows a representative assay from at least three independent experiments. PCR conditions: 94°C 2 min, followed by 27 to 30 cycles of 94°C for 30 s, 55 to 58°C for 30 s, and 72°C for 1 min, followed by 72°C for 5 min. In panel A, bar graphics show qPCR relative product quantification normalized to an endogenous host sequence (e) (accession no. AL833773.6: 11076-5′-GGGTGTTCTTGATCCATTTGG-3′-11058 and 11253-5′-CACACAGC

TABLE 1. MMTV insertion sites found and primers used in this study[a]

Tumor line	MMTV strain-specific and MMTV-specific, non-strain-specific primer sequences	Insertion site position, nearest located gene, and transcriptional orientation with respect to MMTV	Primers for checking presence of cloned insertion sites (MMTV-host)
2216	5′-TCAAATATACTCATGGGGG-3′ [MMTV(LA)]	ChrX, 10 kb downstream to *Rai2*; same orientation	5′-AGTGTAGGACACTCTCGGG-3′
	5′-AGTGTAGGACACTCTCGGG-3′		5′-TACATGCATGGGCTCTTGAAC-3′
2144	5′-TAGTATTAAGGCATTGCCCTTG-3′ [MMTV(BALB-2)]	Chr7, 25 kb upstream to *Int2*/*Fgf3*; opposite orientation	5′-GAGTAAACTTGCAACAGTCC-3′
	5′-AGGAAGGTCGAGTTCTCCG-3′		5′-ACTGTCAACTTAGCACTTGC-3′
2314	5′-TCAAATATACTCATGGGGG-3′ [MMTV(LA)]	Chr7, 3′ noncoding of *Int2*/*Fgf3*; same orientation	5′-GAGTAAACTTGCAACAGTCC-3′
	5′-AGTGTAGGACACTCTCGGG-3′		5′-TGGATGACTTTGAGTCTGGG-3′
2318	5′-ATGATGAGCTTGTGGGGAAAG-3′ [MMTV(BALB-14)]	Chr4, 25 kb upstream to BB640772; same orientation	5′-GAGTAAACTTGCAACAGTCC-3′
	5′-AGGAAGGTCGAGTTCTCCG-3′		5′-GGGTGTTCTTGATCCATTTGG-3′
2318	5′-ATGATGAGCTTGTGGGGAAAG-3′ [MMTV(BALB-14)]	Chr15, 1,400 kb downstream to *Ebag9*; opposite orientation	5′-GAGTAAACTTGCAACAGTCC-3′
	5′-AGGAAGGTCGAGTTCTCCG-3′		5′-TAATGAGTTGCATCCATTTG-3′
D-2	5′-TAGTATTAAGGCATTGCCCTTG-3′ [MMTV(BALB-2)]	Chr8, last intron of *Itgb1*; opposite orientation	5′-AGTGTAGGACACTCTCGGG-3′
	5′-AGGAAGGTCGAGTTCTCCG-3′		5′-GGCTCAGCTCACTTTCTCC-3′
D-2	5′-TAGTATTAAGGCATTGCCCTTG-3′ [MMTV(BALB-2)]	Chr7, 3′ noncoding of *Int2*/*Fgf3*; same orientation	5′-GAGTAAACTTGCAACAGTCC-3′
	5′-AGGAAGGTCGAGTTCTCCG-3′		5′-CCTTGAACTCACAAAGATCC-3′
2312	5′-ATGATGAGCTTGTGGGGAAAG-3′ [MMTV(BALB-14)]	Chr7, 3′ noncoding of *Int2*/*Fgf3*; same orientation	5′-GAGTAAACTTGCAACAGTCC-3′
	5′-AGGAAGGTCGAGTTCTCCG-3′		5′-TGTATTGTCACAGCCTGAAG-3′
2236	5′-TCAAATATACTCATGGGGG-3′ [MMTV(LA)]	Chr4, first intron of *Itgb3bp*; same orientation	5′-GAGTAAACTTGCAACAGTCC-3′
	5′-AGTGTAGGACACTCTCGGG-3′		5′-GTGTATGCAATGGTGTCAGC-3′
2284	5′-TCAAATATACTCATGGGGG-3′ [MMTV(LA)]	Chr10, 2 kb upstream to *Rspo3*; opposite orientation	5′-GAGTAAACTTGCAACAGTCC-3′
	5′-AGTGTAGGACACTCTCGGG-3′		5′-GACAAATCATACTCTGAAAGG-3′

[a] Chr, chromosome no.

9). They included three insertions also observed in all the corresponding PD tumors of the first transplant generation (in tumor lines 2314, D-2, and 2312). Their precise genomic location was determined by "BLATing" the sequence of isolated amplicons in the mouse genome database: http://genome.UCSC.edu (1). The insertion sites were confirmed by PCR analysis using viral/genomic primer pairs (Table 1).

Forty percent (4/10) of isolated insertion sites were located near the *Int2*/*Fgf3* gene, confirming the relevance of these mutations in MMTV-induced PD tumors (7–9, 16). Four other insertion sites were located near genes associated with neoplastic development. They were *Itgb1* (encoding integrin β1), (15, 25), *Rai2* (encoding retinoid acid-induced protein 2) (22–24), *Ebag9* (encoding estrogen receptor-binding fragment-associated protein 9) (19, 21), and *Itgb3bp* (encoding the β3 integrin binding protein β3 endonexin) (2, 18). We have also identified an insertion site 25 kb downstream of locus BB640772 and 2 kb upstream of *Rspo3* (6) of unknown function that contains a thrombospondin type 1 domain 2.

Expression analysis of these loci by semiquantitative reverse transcription-PCR revealed that MMTV insertions near target genes increased their expression (Fig. 2). The common target *Fgf3* is not expressed in normal tissues and was induced in the four tumors with insertions in this locus. In addition, *Fgf3* expression was also up-regulated in 3/4 tumor lines with no detected insertions in that locus. This result indicates that overexpression of this gene is very common in our mammary tumor model.

Expression of *Rspo3* correlated with MMTV insertion near the locus in the tumor line 2284. In addition, *Rspo3* expression was found in tumor line 2216 and, weakly, in 2144. Its expression was not detected in the other tumor lines or in virgin mammary glands. Besides, we found a negative correlation between *Fgf3* and *Rspo3* expression, since 2284 was the only tumor line we found to be negative for *Fgf3* expression and 2216 and 2144 showed lower *Fgf3* expression than the other tumor lines. Interestingly, it has been shown that human Rspo1 induces epithelial cell proliferation and β-catenin stabilization,

TATGGTCACTTG-3′-11273) using 1:30,000 SYBR Green (Molecular Probes, Inc). Proviral MMTV/e, proviral MMTV content relative to endogenous host sequence; a value of 1 was assigned to the sample showing the highest level of proviral MMTV content; au, arbitrary units. In panel B, Southern blot analysis with an MMTV-LTR probe (3, 9) is shown to indicate fragments that have been cloned out by IPCR (big arrows); arrowheads, other MMTV insertion sites that have not been isolated; PD, pregnancy-dependent tumor; PI, pregnancy-independent tumor. Top right corner: MMTV-LTR probe Southern blot analysis showing the endogenous MMTV band pattern from BALB/c mouse spleen DNA digested with EcoRI and HindIII.

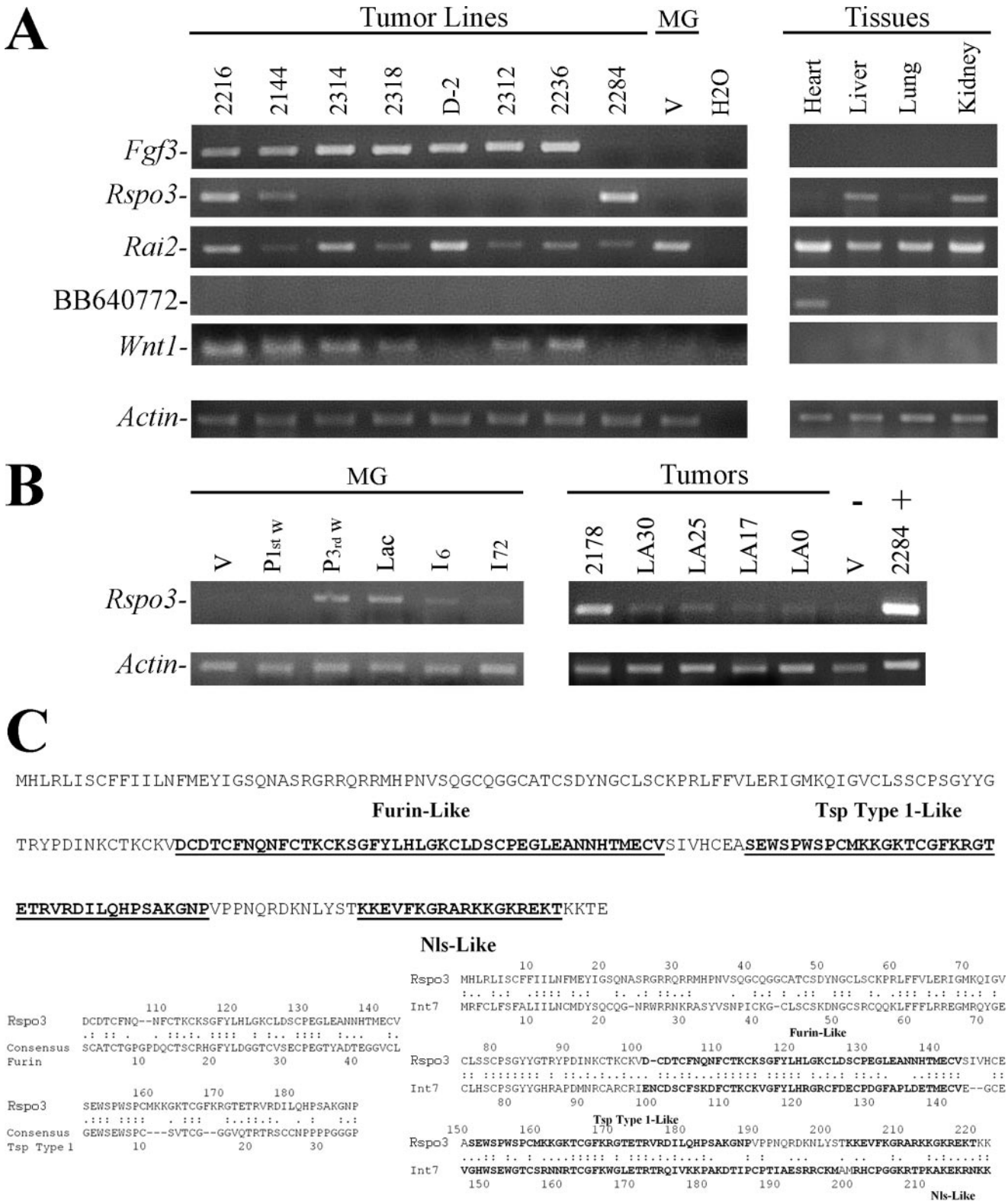

FIG. 2. MMTV insertion sites in mammary tumor lines. (A and B) RT-PCR assays were performed to test the following: (A) Expression of known (*Fgf3* and *Wnt1*) and new (*Rai2*, BB640772, and *Rspo3*) insertion sites in PI transplants of tumor lines listed in Table 1, normal uninfected virgin mammary gland (MG-V), heart, liver, lung, and kidney; (B) *Rspo3* expression in mammary glands (MG) of virgin (V), first week pregnant (P 1st w), third week pregnant (P 3rd w), lactating (Lac), 6 h postlactation (I6), or 72 h postlactation (I72) mice and in five other tumor lines (2178, LA30, LA25, LA17, and LA0); virgin mammary gland (V) and a tumor from line 2284 (2284) were assayed as negative and positive controls, respectively. Assays were performed using total RNA (9, 17) with MMLV retrotranscriptase (Promega), followed by DNA *Taq* polymerase (Invitrogen). PCR conditions: 94°C for 2 min, followed by 30 to 32 cycles of 94°C for 30 s, 58°C for 30 s, 72°C for 1 min, followed by 72°C for 5

possibly by a process that is distinct from the canonical Wnt-mediated signaling pathway (11). In addition, it has been recently reported that all four human Rspo family members induce very similar effects in intestinal epithelium (12). Therefore, taking into account the relevance of Wnt pathway activation in our tumor model (9), it is not surprising that the few cases in which we found lower Wnt-1 and Fgf3 expression (Fig. 2) corresponded to high Rspo3 expression levels, suggesting that in these tumors, this protein might be at least partially responsible for the observed tumor phenotype. Expression analysis of *Rai2* indicated a weak association with the tumor cells. *Rai2* is expressed in all normal tissues analyzed, as well as in the tumor lines, regardless of the location of viral insertion. On the other hand, mRNA from BB640772 was not detected in tumor lines but only in heart tissue (Fig. 2A). When the expression of common insertion sites, such as *Int1*/*Wnt1* and *Int7*, was analyzed, we found that while most tumor lines expressed the former (Fig. 2A), none of them expressed the latter (data not shown).

The expression pattern of *Rspo3* in mammary cells and tumors was further analyzed. We found that late pregnant and lactating mammary glands show weak expression of *Rspo3* transcript. Besides, the screening of five additional independent tumor lines showed another one (i.e., 2178) with *Rspo3* overexpression (Fig. 2B). However, we have not found evidence from the IPCR approach indicating that overexpression of Rspo3 in tumors different from 2284 is due to MMTV insertions. Similar results were obtained when PCRs were performed using the 3′-end and 5′-end MMTV long terminal repeat (MMTV-LTR)-specific primers shown in Table 1 and primers located at the 5′ and 3′ ends of the *Rspo3* coding sequence using E-Longase enzyme mix (Invitrogen) with 12 min of extension in order to detect MMTV insertions up to 10 to 12 kb upstream or downstream of *Rspo3*. These reactions confirmed the MMTV insertion found in tumor line 2284 but in none of the others. Therefore, it is possible that *Rspo3* high expression found in tumors different from 2284 would be due to a secondary effect of other insertions or mutations. Interestingly, analysis of the *Rspo3* coding sequences revealed a surprising similarity to the recently described *Int7* (14). Both proteins contain a nuclear localization signal, as well as a furin-like and a thrombospondin-like domain (Fig. 2C).

As indicated above, the MMTV insertion sites were isolated from PI tumor transplants. To find out whether they occurred early during progression, their presence was tested by PCR analysis in the PD passages from which PI tumors had originated. Our results show that in all cases the mutations were detected in the early transplant generations. In addition, each case that was analyzed by qPCR (7/10) revealed a notable increase in the insertion-specific MMTV subpopulation associated with tumor progression (Fig. 3).

We have previously reported that in the polyclonal PD tumor transplants, long latency periods in virgin hosts lead to the selection of specific cell subpopulations (9). The data shown herein confirm those results. For example, tumor line 2144 showed an increase of the *Int2*/*Fgf3*-associated subpopulation only after undergoing a long dormancy period. Conversely, the subpopulation that expanded rapidly to the PI stage lacked this mutation (Fig. 3B). Similar conclusions can be made from tumor line D-2 (Fig. 3E). Therefore, MMTV insertion in the *Int2*/*Fgf3* locus would be a common initiation event, and the increase of populations containing such mutations may be important for certain progression patterns, such as those that require dormant estrogen receptor-positive, progesterone receptor-positive cells to survive in virgin female hosts.

Interestingly, all the MMTV insertions that were detectable by Southern blot analysis in the PD tumor transplants were located at the *Int2*/*Fgf3* locus (tumor lines 2314, D-2, and 2312; data not shown). These data suggest that cells containing these mutations were quickly selected and rapidly became predominant in polyclonal PD tumor transplants. This idea was confirmed by the qPCR assays, which demonstrated that clones containing these mutations were the only ones showing less than an 80% increase in association with progression towards PI behavior (Fig. 3).

In the two tumor lines harboring two MMTV insertion sites (i.e., 2318 and D-2), the increment of each mutation during progression was very similar to the other one present in the same line (Fig. 2D and E). This suggests that both MMTV insertion events occurred in the same cell and confirms that there is a single progenitor cell from which PI tumors evolve.

In conclusion, this study shows that in the MMTV cancer model, PI tumors progress from the selection of cell populations in PD tumors with specific mutations and suggests that clonal expansion of these cells would be more relevant for progression than occurrence of new insertions. Those early viral insertions might induce oncogene overexpression that could determine selection of specific cell populations during progression. In addition, our results provide new evidence of *Int2*/*Fgf3* relevance in the early development of hormone-dependent mammary tumors, and a new gene, *Rspo3*, is introduced as a candidate oncogene involved in mouse mammary tumor development.

We thank Christiane Dosne Pasqualini and Isabel Piazzon for their support and Antonio Morales and Héctor Costa for their efficient technical assistance. We also thank Robert Callahan (NCI, NIH) for providing us *Int7* primers and positive controls and Omar Coso for his helpful comments on the manuscript.

min. Primers: *Fgf3* (9); *Rspo3* f (5′-GTGTTCTAGCCATTAGTACC-3′) and r (CCACCCTGTACATGGAGC-3′); *Wnt1* (20); *Rai2* f (5′-CCTC CAGTCAAAGGAGTAC-3′) and r (5′-CGGCGTCTTCAACTGACAC-3′); BB640772 f (5′-ACCAGAAAAGGATGTTGTCC-3′) and r (5′-T GGTAGGCCTAAGGAATGC-3′); and actin (17). (C) RSPO3 amino acid sequence. Regions similar to furin (Furin-Like), thrombospondin type 1 (Tsp Type 1-Like), and the nuclear localization (Nls-Like) consensus sequences are underlined and in bold. *Rspo3* comparison with Furin, Tsp Type 1 consensus, and *Int7* (14) is shown below. Motifs were predicted with PROSITE MotifScan (www.expasy.org/prosite), and alignments were carried out using LALIGN (http://fasta.bioch.virginia.edu/fasta/lalign.htm). One point, similarities; two points, identities; -, gaps; Ala, A; Cys, C; Asp, D; Glu, E; Phe, F; Gly, G; His, H; Ile, I; Lys, K; Met, M; Asn, N; Pro, P; Gln, Q; Arg, R; Ser, S; Thr, T; Val, V; Trp, W; Tyr, Y.

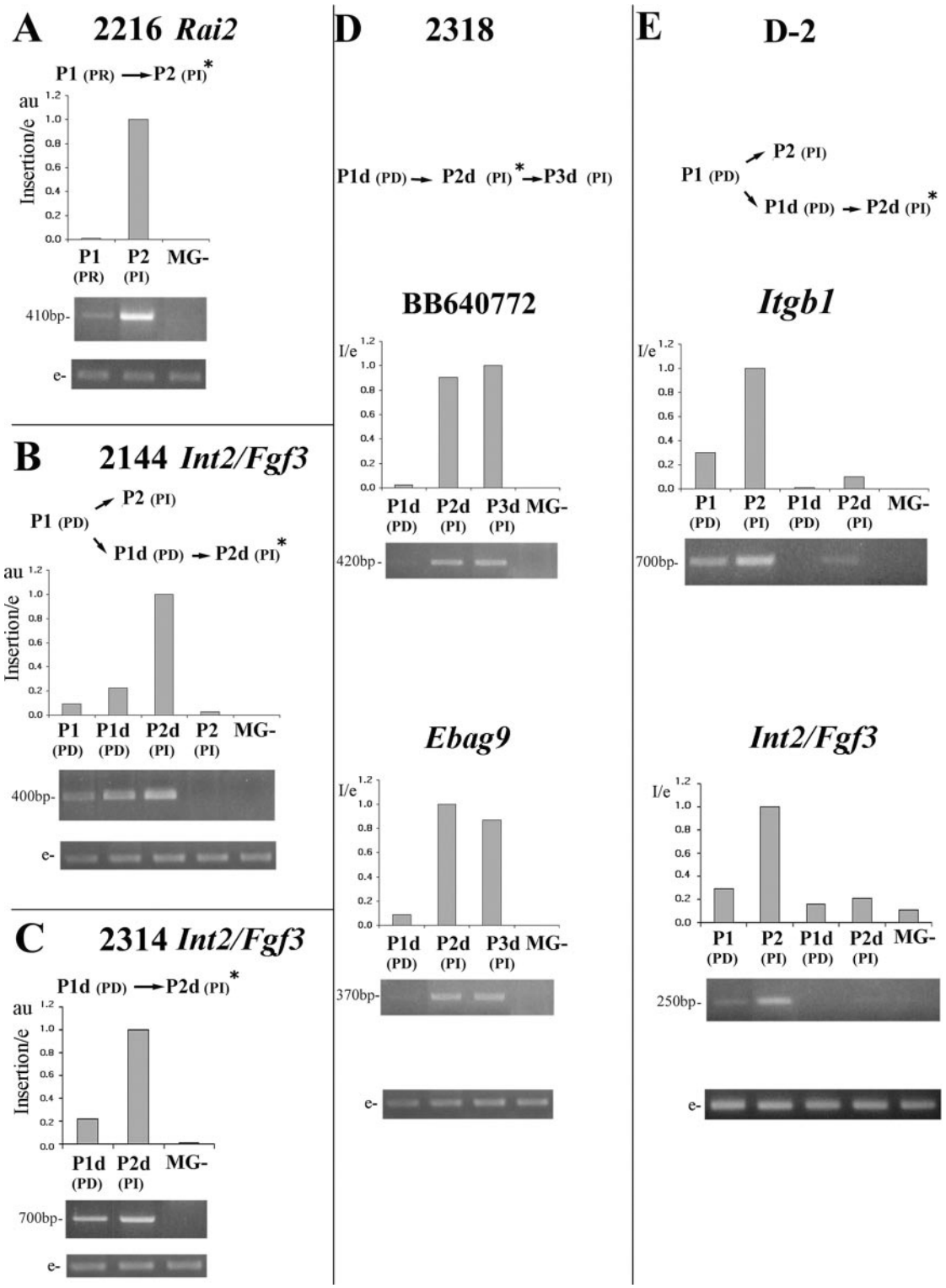

FIG. 3. Relative quantification of MMTV-associated specific mutations. PCR analysis of seven MMTV insertion sites from five independent tumor lines: 2216 (A), 2144 (B), 2314 (C), 2318 (D), and D-2 (E). For 2318 and D-2, two MMTV insertion sites were identified and tested (D and E). At the top of each panel, a schematic representation depicting each tumor line pattern of progression is shown. PCRs were performed with genomic and provirus-LTR-specific primers and normalized as explained in the legend to Fig. 1. Bar graphics indicate template relative quantification by qPCR (each one represents three independent assays). PD, pregnancy-dependent tumor; PI, pregnancy-independent tumor; PDd, pregnancy-dependent tumor that resumed growth after a long dormancy period; PId, pregnancy-independent tumor that arose from a PDd transplantation; PR, pregnancy-responsive tumor; MG-, normal mammary gland from MMTV-uninfected mice. P1, P2, and P3, first, second, and third tumor transplant generations; insertion/e, specific MMTV insertion relative to an endogenous host sequence; a value of 1 was assigned to the sample showing the highest level of each specific insertion in the assayed tumor DNA; au, arbitrary units; *, tumor passage from which proviral insertion site has been isolated; e, endogenous host sequence.

This work was supported by the Fogarty International Center, National Institutes of Health (grant R01TW006212 to E.C.K.), and CONICET, ANPCyT, Fundación Antorchas, LALCEC-Fundación AVON, and Fundación Bunge&Born, Argentina.

REFERENCES

1. **Benson, D. A., I. Karsch-Mizrachi, D. J. Lipman, J. Ostell, and D. L. Wheeler.** 2004. GenBank: update. Nucleic Acids Res. **32:**D23–D26.
2. **Besta, F., S. Massberg, K. Brand, E. Muller, S. Page, S. Gruner, M. Lorenz, K. Sadoul, W. Kolanus, E. Lengyel, and M. Gawaz.** 2002. Role of beta(3)-endonexin in the regulation of NF-kappaB-dependent expression of urokinase-type plasminogen activator receptor. J. Cell Sci. **115:**3879–3888.
3. **Buggiano, V., C. S. Levy, A. Gattelli, M. C. Cirio, M. Marfil, I. Nepomnaschy, I. Piazzon, L. Helguero, S. Vanzulli, and E. C. Kordon.** 2002. Origin and progression of pregnancy-dependent mammary tumors induced by new mouse mammary tumor virus variants. Breast Cancer Res. Treat. **75:**191–202.
4. **Buggiano, V., C. Schere-Levy, K. Abe, S. Vanzulli, I. Piazzon, G. H. Smith, and E. C. Kordon.** 2001. Impairment of mammary lobular development induced by expression of TGFbeta1 under the control of WAP promoter does not suppress tumorigenesis in MMTV-infected transgenic mice. Int. J. Cancer **92:**568–576.
5. **Castilla, L. H., P. Perrat, N. J. Martinez, S. F. Landrette, R. Keys, S. Oikemus, J. Flanegan, S. Heilman, L. Garrett, A. Dutra, S. Anderson, G. A. Pihan, L. Wolff, and P. P. Liu.** 2004. Identification of genes that synergize with Cbfb-MYH11 in the pathogenesis of acute myeloid leukemia. Proc. Natl. Acad. Sci. USA **101:**4924–4929.
6. **Chen, J. Z., S. Wang, R. Tang, Q. S. Yang, E. Zhao, Y. Chao, K. Ying, Y. Xie, and Y. M. Mao.** 2002. Cloning and identification of a cDNA that encodes a novel human protein with thrombospondin type I repeat domain, hPWTSR. Mol. Biol. Rep. **29:**287–292.
7. **Clausse, N., D. Baines, R. Moore, S. Brookes, C. Dickson, and G. Peters.** 1993. Activation of both Wnt-1 and Fgf-3 by insertion of mouse mammary tumor virus downstream in the reverse orientation: a reappraisal of the enhancer insertion model. Virology **194:**157–165.
8. **Clausse, N., R. Smith, C. M. Calberg-Bacq, G. Peters, and C. Dickson.** 1993. Mouse mammary-tumor virus activates Fgf-3/Int-2 less frequently in tumors from virgin than from parous mice. Int. J. Cancer **55:**157–163.
9. **Gattelli, A., M. C. Cirio, A. Quaglino, C. Schere-Levy, N. Martinez, M. Binaghi, R. P. Meiss, L. H. Castilla, and E. C. Kordon.** 2004. Progression of pregnancy-dependent mouse mammary tumors after long dormancy periods. Involvement of Wnt pathway activation. Cancer Res. **64:**5193–5199.
10. **Golovkina, T. V., I. Piazzon, I. Nepomnaschy, V. Buggiano, M. de Olano Velaqq, and S. R. Ross.** 1997. Generation of a tumorigenic milk-borne mouse mammary tumor virus by recombination between endogenous and exogenous viruses. J. Virol. **71:**3895–3903.
11. **Kim, K. A., M. Kakitani, J. Zhao, T. Oshima, T. Tang, M. Binnerts, Y. Liu, B. Boyle, E. Park, P. Emtage, W. D. Funk, and K. Tomizuka.** 2005. Mitogenic influence of human R-spondin1 on the intestinal epithelium. Science **309:**1256–1259.
12. **Kim, K. A., J. Zhao, S. Andarmani, M. Kakitani, T. Oshima, M. E. Binnerts, A. Abo, K. Tomizuka, and W. D. Funk.** 2006. R-Spondin proteins: a novel link to beta-catenin activation. Cell Cycle **5:**23–26.
13. **Kordon, E. C., and G. H. Smith.** 1998. An entire functional mammary gland may comprise the progeny from a single cell. Development **125:**1921–1930.
14. **Lowther, W., K. Wiley, G. H. Smith, and R. Callahan.** 2005. A new common integration site, Int7, for the mouse mammary tumor virus in mouse mammary tumors identifies a gene whose product has furin-like and thrombospondin-like sequences. J. Virol. **79:**10093–10096.
15. **Perlino, E., M. Lovecchio, R. A. Vacca, M. Fornaro, L. Moro, P. Ditonno, M. Battaglia, F. P. Selvaggi, M. G. Mastropasqua, P. Bufo, and L. R. Languino.** 2000. Regulation of mRNA and protein levels of beta1 integrin variants in human prostate carcinoma. Am. J. Pathol. **157:**1727–1734.
16. **Peters, G., A. E. Lee, and C. Dickson.** 1984. Activation of cellular gene by mouse mammary tumour virus may occur early in mammary tumour development. Nature **309:**273–275.
17. **Schere-Levy, C., V. Buggiano, A. Quaglino, A. Gattelli, M. C. Cirio, I. Piazzon, S. Vanzulli, and E. C. Kordon.** 2003. Leukemia inhibitory factor induces apoptosis of the mammary epithelial cells and participates in mouse mammary gland involution. Exp. Cell Res. **282:**35–47.
18. **Shattil, S. J., T. O'Toole, M. Eigenthaler, V. Thon, M. Williams, B. M. Babior, and M. H. Ginsberg.** 1995. Beta 3-endonexin, a novel polypeptide that interacts specifically with the cytoplasmic tail of the integrin beta 3 subunit. J. Cell Biol. **131:**807–816.
19. **Suzuki, T., S. Inoue, W. Kawabata, J. Akahira, T. Moriya, F. Tsuchiya, S. Ogawa, M. Muramatsu, and H. Sasano.** 2001. EBAG9/RCAS1 in human breast carcinoma: a possible factor in endocrine-immune interactions. Br. J. Cancer **85:**1731–1737.
20. **Szeto, W., W. Jiang, D. A. Tice, B. Rubinfeld, P. G. Hollingshead, S. E. Fong, D. L. Dugger, T. Pham, D. G. Yansura, T. A. Wong, J. C. Grimaldi, R. T. Corpuz, J. S. Singh, G. D. Frantz, B. Devaux, C. W. Crowley, R. H. Schwall, D. A. Eberhard, L. Rastelli, P. Polakis, and D. Pennica.** 2001. Overexpression of the retinoic acid-responsive gene Stra6 in human cancers and its synergistic induction by Wnt-1 and retinoic acid. Cancer Res. **61:**4197–4205.
21. **Takahashi, S., T. Urano, F. Tsuchiya, T. Fujimura, T. Kitamura, Y. Ouchi, M. Muramatsu, and S. Inoue.** 2003. EBAG9/RCAS1 expression and its prognostic significance in prostatic cancer. Int. J. Cancer **106:**310–315.
22. **Walpole, S. M., K. T. Hiriyana, A. Nicolaou, E. L. Bingham, J. Durham, M. Vaudin, M. T. Ross, J. R. Yates, P. A. Sieving, and D. Trump.** 1999. Identification and characterization of the human homologue (RAI2) of a mouse retinoic acid-induced gene in Xp22. Genomics **55:**275–283.
23. **Widschwendter, M., A. Widschwendter, T. Welte, G. Daxenbichler, A. G. Zeimet, A. Bergant, J. Berger, J. P. Peyrat, S. Michel, W. Doppler, and C. Marth.** 1999. Retinoic acid modulates prolactin receptor expression and prolactin-induced STAT-5 activation in breast cancer cells in vitro. Br. J. Cancer **79:**204–210.
24. **Zhu, W. Y., C. S. Jones, S. Amin, K. Matsukuma, M. Haque, V. Vuligonda, R. A. Chandraratna, and L. M. De Luca.** 1999. Retinoic acid increases tyrosine phosphorylation of focal adhesion kinase and paxillin in MCF-7 human breast cancer cells. Cancer Res. **59:**85–90.
25. **Zutter, M. M., S. A. Santoro, W. D. Staatz, and Y. L. Tsung.** 1995. Reexpression of the alpha 2 beta 1 integrin abrogates the malignant phenotype of breast carcinoma cells. Proc. Natl. Acad. Sci. USA **92:**7411–7415.